ISSN 1070-4272, Russian Journal of Applied Chemistry, 2016, Vol. 89, No. 3, pp. 489−499. © Pleiades Publishing, Ltd., 2016.

VARIOUS TECHNOLOGICAL PROCESSES

Thermodynamic and Adsorption Behavior of N_2O_4 Schiff Base as a Corrosion Inhibitor for API-5L-X65 Steel in HCl Solution[1]

I. Danaee[a]* and N. Bahramipanah[b]

[a]*Abadan Faculty of Petroleum Engineering, Petroleum University of Technology, Abadan, Iran*
[b]*Department of Chemistry, Payame Noor University, P.O.BOX 19395-3697, Tehran, Iran*
**e-mail: danaee@put.ac.ir*

Received February 4, 2016

Abstract—The inhibition ability of *N,N*'-bis(2,4-dihydroxyacetophenone)-1,3-propandiimine (DHAPP) as a schiff base against the corrosion of API-5L-X65 in 1 M HCl solution was evaluated by polarization, electrochemical impedance spectroscopy, and scanning electron microscopy. Polarization studies indicated that DHAPP retards both the cathodic and anodic reactions through chemical adsorption and blocking the active corrosion sites. The adsorption of this compound obeyed the Langmuir adsorption isotherm. The inhibition efficiency increased with inhibitor concentration and decreased with increasing temperature. EIS data analysed to equivalent circuit model showed that as the inhibitor concentration increased the charge transfer resistance of steel increased whilst double layer capacitance decreased. Kinetic and thermodynamic parameters such as activation energy, enthalpy, entropy, and Gibbs free energy of activation and adsorption were calculated. Gibbs free energy indicated that adsorption occurred through physical and spontaneous process. Scanning electron microscopy was used to study the steel surface with and without inhibitor.

DOI: 10.1134/S10704272160030216

The inhibition ability of *N,N*'-bis(2,4-dihydroxyacetophenone)-1,3-propandiimine (DHAPP) as a schiff base against the corrosion of API-5L-X65 in 1 M HCl solution was evaluated by polarization, electrochemical impedance spectroscopy, and scanning electron microscopy. Polarization studies indicated that DHAPP retards both the cathodic and anodic reactions through chemical adsorption and blocking the active corrosion sites. The adsorption of this compound obeyed the Langmuir adsorption isotherm. The inhibition efficiency increased with inhibitor concentration and decreased with increasing temperature. EIS data analysed to equivalent circuit model showed that as the inhibitor concentration increased the charge transfer resistance of steel increased whilst double layer capacitance decreased. Kinetic and thermodynamic parameters such as activation energy, enthalpy, entropy, and Gibbs free energy of activation and adsorption were calculated. Gibbs free energy indicated that adsorption occurred through physical and spontaneous process. Scanning electron microscopy was used to study the steel surface with and without inhibitor.

INTRODUCTION

Even with advanced corrosion resistant materials available, steel has been widely employed as construction materials for pipe work in the oil and gas production such as down hole tubular, flow lines, and transmission pipelines [1]. API 5L X65 steel is the most widely accepted material for these types of pipes [2, 3]. Steel pipelines play an important role in transporting gases and liquids throughout the world. Acid solutions are widely used in industries for lots of purposes, such as acid pickling, industrial acid cleaning, acid descaling, and oil well acidizing [4, 5]. The general aggressive nature of acid solutions leads to corrosive attack. Massive costs are invested to manage corrosion in the oil and gas industry. The strategies consist either in using corrosion resistant alloys or the use of steel with corrosion inhibitor [6, 7].

[1] The text was submitted by the authors in English.

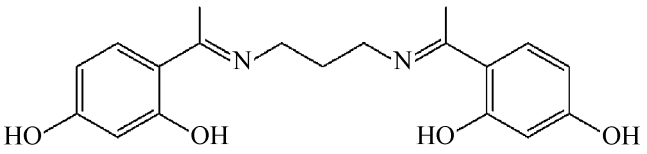

Fig. 1. Chemical structure of DHAPP.

Inhibition of organic compound inhibitors occurs due to interaction between inhibitor molecules and the metal surface via adsorption. The inhibitor adsorption depends on parameters such as the surface charge and nature of the metal, the inhibitor structure, aggressive media type, and the extent of aggressiveness and also on the nature of its interaction with metal surface [8, 9]. Generally the organic compounds containing hetero atoms like O, N, S, and P are found to work as very effective corrosion inhibitors [10, 11]. The choice of the inhibitor is based on two considerations, firstly, economic consideration and, secondly, high inhibition efficiency. Both features obviously can be combined within the same molecule such as Schiff bases [12–15]. In the past few years, the corrosion inhibition of various metals such as aluminum, and of steel in acid solutions by Schiff bases with environmental considerations has attracted more attention [16, 17]. Schiff bases can conveniently be synthesized from relatively cheap starting materials, an amine and a ketone or aldehyde. It was also reported that Schiff bases show more inhibition efficiency than corresponding amine [18, 19].

The work is devoted to study the inhibition characteristics of *N,N*'-bis(2,4-dihydroxyacetophenone)-1,3-propandiimine as an inhibitor for steel in HCl solution, using potentiodynamic polarization measurements (Tafel), electrochemical impedance spectroscopy (EIS), and scanning electron microscopy. Thermodynamic parameters such as enthalpy, entropy, and Gibbs free energy were calculated from experimental data of the inhibition process at different temperature.

EXPERIMENTAL

Materials. API-5L-X65 samples were cut from parent pipe with chemical composition reported as C 0.12, Mn 1.3, Si 0.22, Cr 0.25, Mo 0.18, Cu 0.12, Ni 0.1, P 0.01, S 0.003, Al 0.02, Nb 0.05, Sn 0.01, V 0.05, Ti 0.005, and Fe rest. The specimens of dimension 1 cm × 1 cm (exposed) × 4.3 mm (isolated with polyester resin) were used for electrochemical methods. They were polished mechanically using different grade emery papers up to 2000, washed thoroughly with doubly distilled water, and degreased with acetone before being immersed in the acid solution.

The DHAPP Schiff base inhibitor (Fig. 1) was provided in high yield (96%) by the condensation of 2,4-dihydroxyacetophenone (2 mmol) with 1,3-diaminopropane (1 mmol) in a stirred ethanolic solution and heated to reflux for 4 h according to the procedure described in [20]. The resulting precipitate was filtered off, washed with warm ethanol, and diethyl ether. Identification of structure of synthesized Salen ligand was performed by IR and ^{1}H NMR spectroscopy and elemental analysis. The concentration range of inhibitor employed was varied from 1×10^{-4} to 2×10^{-3} M.

Apparatus and methods. The apparatus for electrochemical investigations consists of a computer controlled Auto Lab potentiostat/galvanostat (PGSTAT302N) electrochemical measurement system at a scan rate of 1 mV s^{-1}. The electrochemical experiments were carried out using a conventional three electrode cell assembly at 20 ± 2°C. A rectangular platinum foil was used as counter electrode and saturated calomel electrode as the reference electrode. The EIS experiments were conducted in the frequency range of 100 kHz to 0.01 Hz at open circuit potential. The AC potential amplitude was 10 mV. Time interval of 20–25 min was given for steady state attainment of open circuit potential. Fitting of experimental impedance spectroscopy data to the proposed equivalent circuit was done by means of home written least square software based on Marquardt method for the optimization of functions and Macdonald weighting for the real and imaginary parts of the impedance [21, 22].

For surface analysis, the specimens were immersed in 1 M HCl prepared with and without addition of 1×10^{-3} M of DHAPP at 20 ± 2°C for 6 h, cleaned with distilled water. The surface morphology of the electrode surface was evaluated by scanning electron microscopy (VEGA\ TESCAN).

RESULTS AND DISCUSSION

Electrochemical results. Polarization curves were obtained for steel electrode in 1 M HCl solution with and without inhibitor. The polarization exhibits Tafel behavior. Tafel lines which were obtained at various concentrations of DHAPP in 1 M HCl solutions were presented in Fig. 2,

at 20°C. The corresponding electrochemical parameters, i.e., corrosion potential (E_{corr} vs. SCE), corrosion current density (I_{corr}), cathodic and anodic Tafel slopes (β_a,β_c), the degree of surface coverage (θ) and the inhibition efficiency (IE% = $\theta \times 100$) were obtained by extrapolation of the Tafel lines and are shown in Table 1. The degree of surface coverage for different concentrations of inhibitor is calculated using the following equation [23, 24]:

$$\theta = \frac{I - \dot{I}}{I}, \quad (1)$$

where I and $\dot{I}$ are the corrosion current densities without and with corrosion inhibitor, respectively. The addition of DHAPP shifts both anodic and cathodic branches to the lower values of corrosion current densities and, thus, causes a remarkable decrease in the corrosion rate. It can be clearly seen from Fig. 2 that, as would be expected, both anodic metal dissolution of iron and cathodic hydrogen ions reduction reactions are inhibited after the addition of schiff base to the aggressive solution. These results are indicative of the adsorption of inhibitor molecules on the active sites of carbon steel surface [25]. The inhibition of both anodic and cathodic reactions increases with the increasing inhibitor concentrations. The fact that cathodic current–potential curves give rise to parallel lines indicates that the addition of DHAPP to the 1 M HCl solution does not modify the reduction mechanism and the reduction at steel suface takes place mainly through a charge transfer mechanism [26–28]. The slopes do not display an order with the inhibitor concentration. This feature demonstrates that inhibition occurred by a blocking mechanism on the available metal spaces [29–32]. The corrosion potential shows a small change in the range of –501 to –508 mV vs. SCE and the curves change slightly towards the negative direction. These results indicated that the presence of DHAPP compound

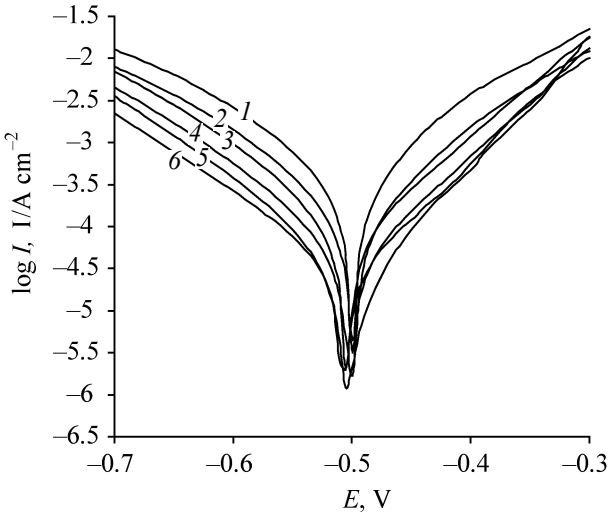

Fig. 2. Anodic and cathodic polarization curves of steel in 1 M HCl without and with various concentration of DHAPP at 25°C: (*1*) 0, (*2*) 1×10^{-4}, (*3*) 3×10^{-4}, (*4*) 5×10^{-4}, (*5*) 1×10^{-3}, (*6*) 2×10^{-3} M.

inhibits iron oxidation and the hydrogen evolution reaction. Consequently these compounds can be classified as the mixed corrosion inhibitors, as electrode potential displacement is lower than 85 mV in any direction [33]. It can be seen in anodic domain that when the scan process proceeds to potentials higher than –320 mV the current densities start to increase and approach to without inhibitor diagram, suggesting that the inhibitors start to desorbs. The polarization resistance (R_p) from Tafel extrapolation method is calculated using the Stern–Geary equation [34]:

$$R_p = \frac{\beta_a \beta_c}{2.303(\beta_a + \beta_c)} \times \frac{1}{I_{corr}}, \quad (2)$$

By increasing the inhibitor concentration, the polarization resistance increases in the presence of

Table 1. Potentiodynamic polarization parameters for the corrosion of steel in 1 M HCl solution in absence and presence of different concentrations of DHAPP at 20 °C

Concentration, M	I_{corr}, μA cm^{-2}	$-E_{corr}$, V	β_a, V dec^{-1}	β_c, V dec^{-1}	R_p, m^{-2}	θ	IE %
Blank	323	–0.501	0.105	–0.102	69.42	–	–
1×10^{-4}	181	–0.501	0.112	–0.095	122.65	0.43	43
3×10^{-4}	104	–0.506	0.108	–0.085	197.23	0.67	67
5×10^{-4}	63	–0.503	0.099	–0.091	326.31	0.80	80
1×10^{-3}	38	–0.508	0.123	–0.109	644.98	0.87	87
2×10^{-3}	24	–0.505	0.125	–0.116	1064.28	0.92	92

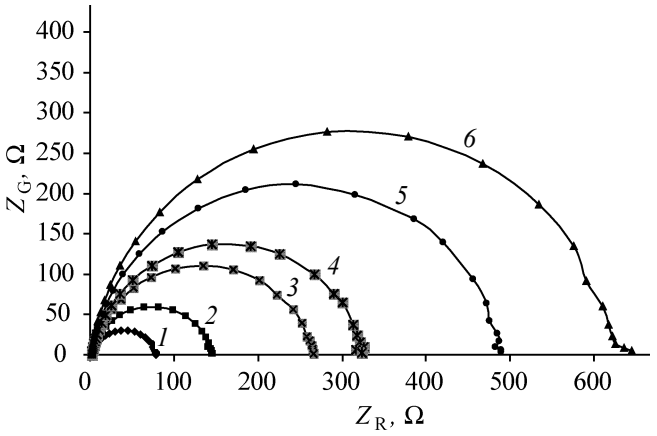

Fig. 3. Nyquist plots for steel in 1 M HCl without and with various concentration of DHAPP at 25°C: (*1*) 0, (*2*) 1 × 10–4, (*3*) 3 × 10–4, (*4*) 5 × 10–4, (*5*) 1 × 10–3, (–) 2 × 10–3 M.

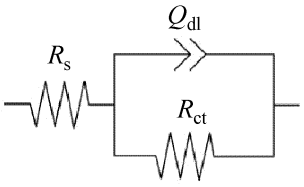

Fig. 4. Equivalent circuits compatible with the experimental impedance data in Fig. 3 for corrosion of steel electrode at different inhibitor concentrations.

compound, indicating adsorption of the inhibitor on the metal surface to block the active sites efficiently and inhibit corrosion [35].

Figure 3 shows the Nyquist diagrams of API-5L-X65 in 1 M HCl solutions containing different concentrations of DHAPP. All the impedance spectra exhibit single depressed semicircle. The diameter of semicircle increases with the increase in DHAPP concentrations. The semicircular appearance shows that the corrosion of carbon steel is controlled by the charge transfer and the presence of DHAPP does not change the mechanism of carbon steel dissolution [36, 37]. In addition, these Nyquist diagrams are not perfect semicircles. The deviation of semicircles from perfect circular shape is often referred to the frequency dispersion of interfacial impedance [37–39]. This behavior is usually attributed to the inhomogeneity of the metal surface arising from surface roughness or interfacial phenomena [39, 40], which is typical of solid metal electrodes [41]. The equivalent circuit compatible with the Nyquist diagram recorded in the presence of inhibitor is depicted in Fig. 4. The simplest approach requires the theoretical transfer function $Z(\omega)$ to be represented by a parallel combination of a resistance R_{ct} and a capacitance C, both in series with another resistance R_s [42]:

$$Z(\omega) = R_s + \frac{1}{\frac{1}{R_{ct}} + i\omega C}, \quad (3)$$

where ω is the frequency in rad/s, $\omega = \pi f$ and f is frequency in Hz. To obtain a satisfactory impedance simulation of steel, it is necessary to replace the capacitor (C) with a constant phase element (CPE) Q in the equivalent circuit. The most widely accepted explanation for the presence of CPE behavior and depressed semicircles on solid electrodes is microscopic roughness causing an inhomogeneous distribution in the solution resistance as well as in the double layer capacitance [43]. Constant phase element Q_{dl}, R_s, and R_{ct} can be corresponded to double layer capacitance $Q_{dl} = R^{n-1}C_{dl}^{n}$, solution resistance and charge transfer resistance, respectively. To corroborate the equivalent circuit, the experimental data are fitted to equivalent

Table 2. Impedance data for mild steel in 1 M HCl solution without and with different concentration of DHAPP at 25°C

Concentration, M	R_s, Ω cm^2	R_{ct}, Ω cm^2	Q_{dl}, F cm^{-2}	C_{dl}, F cm^{-2}	n
Blank	1.9	77	0.0019	0.0013	0.85
1 × 10–5	1.9	144	0.0017	0.0013	0.88
3 × 10–5	1.9	264	0.0014	0.0012	0.89
5 × 10–5	2	322	0.0013	0.0011	0.90
1 × 10–4	2.1	488	0.0010	0.0009	0.91
2 × 10–4	2.1	621	0.0009	0.0008	0.93

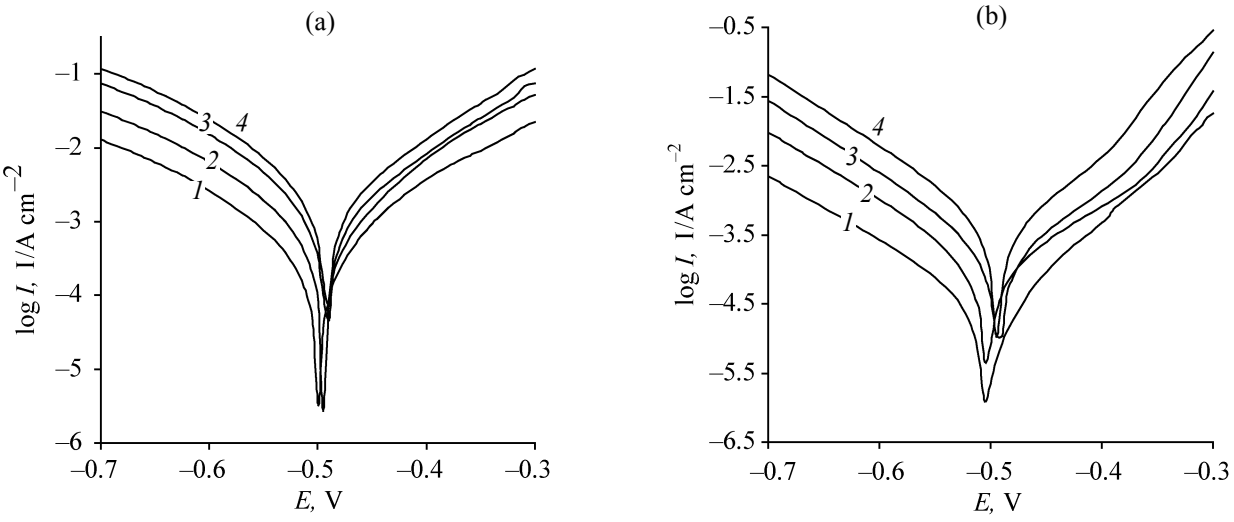

Fig. 5. Anodic and cathodic polarization curves of steel [in (a) 1 M HCl and (b) blank] in presence of 2×10^{-3} M of DHAPP, at different temperatures, °C: (*1*) 20, (*2*) 40, (*3*) 60, and (*4*) 80.

circuit and the circuit elements are obtained. Table 2 illustrates the equivalent circuit parameters for the impedance spectra of corrosion of steel in 1 M HCl solution. The charge transfer resistance increases with increasing inhibitor concentrations due to the higher inhibition efficiencies. The data indicate that increasing charge transfer resistance is associated with a decrease in the double layer capacitance. The decrease in Q_{dl} values is caused by adsorption of inhibitor indicating that the exposed area decreases. On the other hand, a decrease in Q_{dl}, which can be resulted from a decrease in local dielectric constant and/or an increase in the thickness of the electrical double layer, suggests that the inhibitor acts by adsorption at the metal–solution interface and the formation of a protective layer on the electrode surface [37]. The thickness of this protective layer increases with the increase in inhibitor concentration, since more of the inhibitor will electrostatically adsorb on the electrode surface. This trend is in accordance with Helmholtz model, given by the following equation [15, 37]:

$$C_{dl} = \frac{\varepsilon_0 \varepsilon S}{e}, \quad (4)$$

where e is the thickness of the protective layer, ε is the dielectric constant of the medium, ε_0 is the vacuum permittivity, and S is the effective surface area of the electrode.

Since the Q_{dl} exponent (n) is a measure of the surface heterogeneity, values of n indicates that the steel surface becomes more and more homogeneous as the concentration of inhibitor increases as a result of its adsorption on the steel surface and corrosion inhibition. The increase in values of R_{ct} and the decrease in values of Q_{dl} with increasing the concentration also indicate that inhibitor acts as primary interface inhibitor and the charge transfer controls the corrosion of steel under the open circuit conditions.

Effect of temperature. Temperature has a considerable influence on the rate of corrosion. Generally, in acidic medium the corrosion rate increases with temperature because the steel dissolution and hydrogen evolution over potential decrease [20]. To examine the ability of Schiff bases on inhibition of steel corrosion at higher temperatures, polarization were carried out at different temperatures. The change of the corrosion current with the temperature in 1 M HCl both in the absence and in the presence of DHAPP at the temperatures 20, 40, 60, and 80°C are given in Figs. 5a, 5b. The various electrochemical parameters are calculated from Tafel plots and summarized in Tables 3–5. As can be seen, raising the temperature has no significant effect on the corrosion potentials; but leads to a higher corrosion current densities I_{corr}. It is seen that the investigated DHAPP have inhibiting properties at all the studied temperatures and the values of inhibition efficiency for DHAPP decrease with increasing temperature. Thus, the DHAPP inhibitors efficiencies are temperature-dependent. The activation parameters for the corrosion

Table 3. Electrochemical parameters for the corrosion of steel in 1 M HCl solution in absence and presence of different concentrations of DHAPP at 40°C

Concentration, M	I_{corr}, μA cm^{-2}	$-E_{corr}$, V	β_a, V dec^{-1}	β_c, V dec^{-1}	R_p, Ω cm^{-2}	θ	IE %
Blank	602	–0.495	0.111	–0.97	71.77	–	–
1×10^{-4}	416	–0.498	0.124	–0.102	58.29	0.31	31
3×10^{-4}	281	–0.502	0.124	–0.107	88.49	0.53	53
5×10^{-4}	177	–0.501	0.121	–0.89	260.09	0.70	70
1×10^{-3}	112	–0.503	0.118	–0.92	404.74	0.81	81
2×10^{-3}	66	–0.505	0.106	–0.101	339.91	0.89	89

Table 4. Electrochemical parameters for the corrosion of steel in 1 M HCl solution in absence and presence of different concentrations of DHAPP at 60°C

Concentration, M	I_{corr}, μA cm^{-2}	$-E_{corr}$, V	β_a, V dec^{-1}	β_c, V dec^{-1}	R_p, Ω cm^{-2}	θ	IE %
Blank	871	–0.491	0.119	–0.101	27.23	–	–
1×10^{-4}	645	–0.496	0.104	–0.92	62.83	0.25	25
3×10^{-4}	524	–0.499	0.123	–0.96	90.21	0.39	39
5×10^{-4}	389	–0.492	0.134	–0.83	128.76	0.55	55
1×10^{-3}	263	–0.493	0.129	–0.94	187.26	0.69	69
2×10^{-3}	186	–0.495	0.118	–0.99	245.85	0.78	78

Table 5. Electrochemical parameters for the corrosion of steel in 1 M HCl solution in absence and presence of different concentrations of DHAPP at 80°C

Concentration, M	I_{corr}, μA cm^{-2}	$-E_{corr}$, V	β_a, V dec^{-1}	β_c, V dec^{-1}	R_p, Ω cm^{-2}	θ	IE %
Blank	1258	–0.490	0.114	–0.88	34.81	–	–
1×10^{-4}	1023	–0.494	0.107	–0.97	40.89	0.18	18
3×10^{-4}	831	–0.498	0.125	–0.91	57.37	0.33	33
5×10^{-4}	645	–0.490	0.101	–0.99	61.63	0.48	48
1×10^{-3}	489	–0.495	0.131	–0.85	100.63	0.61	61
2×10^{-3}	354	–0.498	0.12	–0.92	129.91	0.71	71

process are calculated from Arrhenius-type plot according to the following equation [20, 44]:

$$\ln I_{corr} = \ln A - \frac{E_a}{RT}, \quad (5)$$

where E_a is the apparent activation corrosion energy, R is the universal gas constant, A is the pre-exponential factor and T is the absolute temperature. Arrhenius plots for the corrosion current density of steel in different concentrations of DHAPP are given in Fig. 6. Values of apparent activation energy of corrosion (E_a) for steel in 1 M HCl without and with various concentrations of DHAPP are determined from the slope of ln I_{corr} versus T^{-1} plots and shown in Table 6. Inspection of the data shows that the activation energy is lower in the absence of inhibitors than in its presence. It was reported that higher

Table 6. Activation parameters of the dissolution of steel in 1 M HCl solution in the absence and presence of DHAPP

Concentration, M	E_a, kJ mol^{-1}	A, A cm^{-2}	ΔH_a, J mol^{-1}	ΔS_a, J mol^{-1} K^{-1}	$E_a - \Delta H_a = RT$, kJ mol^{-1}
Blank	19.2	1.11	16.53	–254.75	2.66
1×10^{-4}	24.3	4.17	21.63	–241.86	2.66
3×10^{-4}	29.6	21.75	26.95	–228.14	2.66
5×10^{-4}	33.5	65.36	30.90	–219.01	2.66
1×10^{-3}	36.4	130.32	33.81	–213.43	2.66
2×10^{-3}	38.9	219.20	36.32	–208.94	2.66

E_a in presence of inhibitor for steel in comparison with blank solution is typically an evidence of physisorption [45]. An alternative formulation of Arrhenius is transition state equation [46]:

$$I_{corr} = \frac{RT}{Nh} \exp \frac{\Delta S_a}{R} \exp \frac{-\Delta H_a}{RT}, \quad (6)$$

where h is Planck's constant, N is Avogadro's number, ΔS_a is the entropy of activation, and ΔH_a is the enthalpy of activation. Figure 7 shows a plot of ln ($I_{corr}T^{-1}$) against T^{-1}. Straight lines are obtained with a slope of ($-\Delta H_a R^{-1}$) and an intercept of ln ($RN^{-1}h^{-1}$) + $\Delta S_a R^{-1}$ from which the values of ΔH_a and ΔS_a are calculated and listed in Table 6. The positive signs of the enthalpies ΔH_a reflect the endothermic nature of the steel dissolution process. Practically E_a and ΔH_a are of the same order. The negative values of entropies ΔS_a imply that the activated complex in the rate determining step represents an association rather than a dissociation step, meaning that a decrease in disordering takes place on going from reactants to the activated complex [47, 48].

Adsorption Isotherm and Thermodynamic Parameters

Adsorption isotherms provide information about the interaction of the adsorbed molecules with the metal surface [25]. The efficiency of Schiff base molecules as a successful corrosion inhibitor mainly depends on their adsorption ability on the metal surface. The adsorption process consists in the replacement of water molecules at a corroding interface according to following process [49]:

$$Org_{(sol)} + nH_2O_{(ads)} \rightarrow Org_{(ads)} + nH_2O_{(sol)}, \quad (7)$$

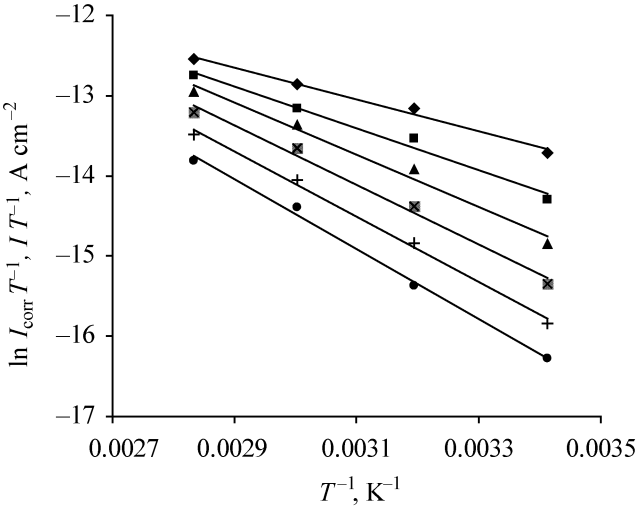

Fig. 6. Typical Arrhenius plots of ln I_{corr} vs. T^{-1} for API 5L B carbon steel in 1 M HCl at different concentrations of DHAPP: (♦) 0, (■) 1×10^{-4}, (▲) 3×10^{-4}, (×) 5×10^{-4}, (+) 1×10^{-3}, (●) 2×10^{-3} M.

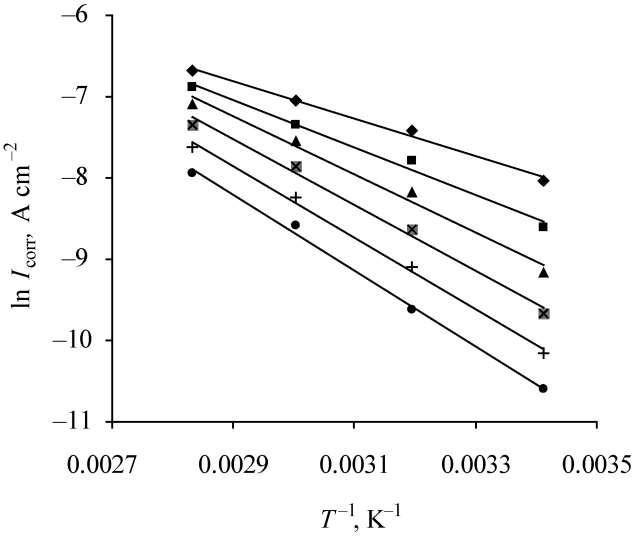

Fig. 7. Typical Arrhenius plots of ln $I_{corr}T^{-1}$ vs. T^{-1} for API 5L B carbon steel in 1 M HCl at different concentrations of DHAPP: (♦) 0, (■) 1×10^{-4}, (▲) 3×10^{-4}, (×) 5×10^{-4}, (+) 1×10^{-3}, (●) 2×10^{-3} M.

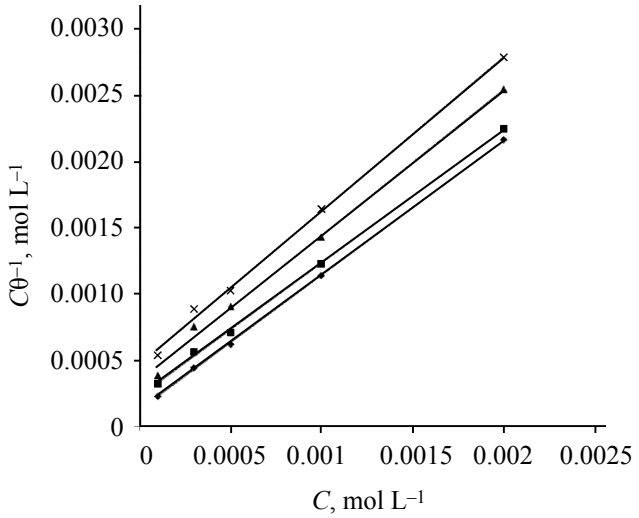

Fig. 8. Langmuir adsorption plot for steel electrode in 1 M HCl at different temperatures, °C: (♦) 20, (■) 40, (▲) 60, and (×) 80.

where $Org_{(sol)}$ and $Org_{(ads)}$ are the organic molecules in the solution and adsorbed onto the metal surface, respectively, and n is the number of water molecules replaced by the organic molecules. It is essential to know the mode of adsorption and the adsorption isotherm that can give important information on the interaction of inhibitor and metal surface. Different adsorption isotherms (Langmuir, Temkin, Freundlich, Frumkin, Modified Langmuir, Henry, Viral, Damaskin, Volmer and Flory–Huggins) [50,51] were tested for their fit to the experimental data. The linear regression coefficient values (R^2) determine from the plotted curves. According to these results, it can be concluded that the best description of the adsorption behavior of DHAPP can be explained by Langmuir adsorption isotherm which is given by:

$$\frac{C}{\theta} = \frac{1}{K_{ads}} + C, \quad (8)$$

where θ is the surface coverage degree, C is the concentration of inhibitor and K_{ads} is the adsorptive equilibrium constant. The linear relationships of $C\theta^{-1}$ versus C, depicted in Fig. 8 suggest that the adsorption of DHAPP on the steel surface obey the Langmuir adsorption isotherm in different temperatures. Langmuir's isotherm assumes that the adsorption of organic molecule on the adsorbent is monolayer and the adsorbed molecules occupy only one site and there are no interactions with other adsorbed species. The standard free energy of adsorption of inhibitor (ΔG_{ads}) on steel surface can be evaluated with the following equation:

$$\Delta G_{ads} = -RT \ln (55.5 K_{ads}), \quad (9)$$

The value 55.5 in the above equation is the concentration of water in solution in mol.l-1 [20]. The negative values of ΔG_{ads} suggest that the adsorption of DHAPP onto the steel surface is spontaneous. Generally, the values of ΔG_{ads} around or less than –30 kJ mol^{-1} are associated with the electrostatic interaction between charged molecules and the charged metal surface (physisorption); while those around or higher than –40 kJ mol^{-1} mean charge sharing or transfer from the inhibitor molecules to the metal surface to form a coordinate type of metal bond (chemisorption). The values of K_{ads} and ΔG_{ads} are listed in Table 7. The ΔG_{ads} values are around –30 kJ mol^{-1}, which means that the absorption of DHAPP onto the steel surface belongs to the physisorption and the adsorptive film has an electrostatic character [18, 20]. The enthalpy and entropy of adsorption (ΔH_{ads} and ΔS_{ads}) can be calculated using the following Gibbs equation [20]:

$$\Delta G_{ads} = \Delta H_{ads} - T\Delta S_{ads}, \quad (10)$$

where ΔH_{ads} and ΔS_{ads} are the variation of enthalpy and entropy of the adsorption process, respectively. A plot of ΔG_{ads} versus T gives a straight line with a slope of $-\Delta S_{ads}$ and an intercept of ΔH_{ads}. The calculated values of ΔH_{ads} and ΔS_{ads} are –22.49 kJ mol^{-1} and 0.033 kJ mol^{-1} K^{-1}. The positive sign of ΔH_{ads} reveals that the adsorption of inhibitor molecules is an endothermic process and the negative value suggests exothermic adsorption. Generally, an exothermic adsorption process suggests either physisorption or chemisorption while endothermic process is attributed to chemisorption [14, 20]. When the process of adsorption is exothermic, physisorption can be distinguished from chemisorptions according to the absolute value of ΔH_{ads}. For physisorption processes, this is usually lower than –40 kJ mol^{-1} while its value is around –100 kJ mol^{-1} for chemisorptions. Based on the results of the present work

Table 7. Equilibrium adsorption parameters for adsorption DHAPP on steel surface in 1 M HCl solution

Temperature, K	$K_{ads} \times 10^{-3}$, L mol^{-1}	ΔG_{ads}, kJ mol^{-1}
298	10	–32.22
313	5	–32.61
333	3	–33.57
353	2	–34.09

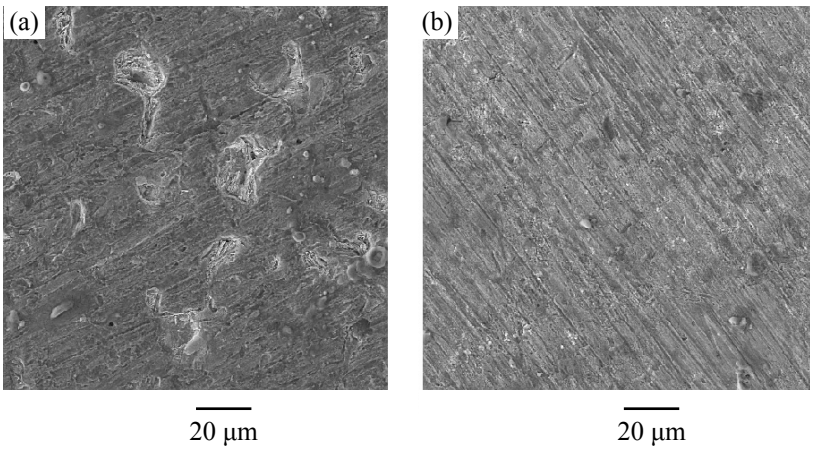

Fig. 9. Surface of steel electrode by SEM microscope at in 1 M HCl solution : (a) without and (b) with 1×10^{-3} M DHAPP.

the calculated ΔG_{ads} and ΔH_{ads} values for DHAPP show that adsorption mechanism is physisorption.

The values of ΔS_{ads} in the presence of DHAPP are positive, meaning that an increase in disordering takes place in going from reactants to the metal-adsorbed species which arises from substitution process, and can be attributed to the increase in the solvent entropy and more positive water desorption entropy. It is also interpreted by an increase of disorders due to the greater amount of water molecules which can be desorbed from the metal surface by one inhibitor molecule [14, 20]. Also entropy ΔS_{ads} and the enthalpy ΔH_{ads} of adsorption can be calculated from the following integrated van't Hoff equation [6, 14]:

$$\ln K_{ads} = -\frac{-\Delta H^{\circ}_{ads}}{RT} + \frac{-\Delta S^{\circ}_{ads}}{R} + \ln \frac{1}{55.5}, \qquad (11)$$

The plot of $\ln K_{ads}$ versus T^{-1} shows straight line for adsorption of DHAPP on steel surface with a slope of $(-\Delta H_{ads}R^{-1})$ and intercept of $[-\ln (55.5)+\Delta S_{ads} R^{-1}]$. The calculated values of ΔH_{ads} and ΔS_{ads} are –22.54 kJ mol^{-1} and 0.032 kJ mol^{-1} K^{-1}. It can be seen that the value of enthalpy of adsorption in Gibbs equation agrees with the one obtained using van't Hoff equation.

Surface Studies

In order to evaluate the conditions of the steel surfaces in contact with hydrochloric acid solution, surface analysis was carried out. Surface was observed before and after 6 h of immersion in 1 M HCl in the absence and presence of DHAPP at 20°C. Scanning electron microscopy (SEM) images of the surface in the absence and presence of inhibitor are presented in Fig. 9. The SEM reveals the presence of corrosion attack and some pits on the surface in the absence of inhibitor while such damages are diminished in the presence of inhibitor. As can be seen from these figures, it is obvious that the surface looks more uniform in the presence of inhibitor.

CONCLUSIONS

The Schiff base was synthesized and investigated as corrosion inhibitor for API-5L-X65 steel in 1 M HCl solution with different concentrations using a series of techniques. The following conclusions were drawn:

(1) Schiff base had an high inhibition effect for the corrosion of API-5L-X65 steel in 1 M HCl solution especially in high concentration. The high inhibition efficiency of Schiff base attributed to the formation of a film on the steel surface.

(2) Polarization measurements demonstrate that Schiff base behaved as mixed type corrosion inhibitor by inhibiting both anodic metal dissolution and cathodic reaction.

(3) Impedance measurements indicated that with increasing inhibitor concentration, the polarization resistance increased, while the double-layer capacitance decreased.

(4) The adsorption of Schiff base molecules on steel surface has been described by Langmuir adsorption isotherm. The values of ΔG_{ads} and K_{ads} indicated the spontaneous interaction with surface and high adsorption ability of studied inhibitor.

(5) The scanning electron microscopy micrographs showed that the corrosion of steel in 1 M HCl solution described by corrosion attack and the addition of inhibitor to the aggressive solutions diminished the corrosion of steel.

REFRERENCES

1. Tyusenkov , A.S. and Cherepashkin, S.E., *Russ. J. Appl. Chem.* 2014, vol. 87, p. 1240.
2. Hegazy, M.A., Abdallah, M., Awad, M.K., and Rezkm, M., *Corros. Sci.,* 2014, vol. 81, p. 54.
3. Migahed, M.A., Al-Sabagh, A.M., Khamis, E.A., and Zaki, E.G., *J. Mol. Liq.,* 2015, vol. 212, p. 360.
4. Zhu, L., Yang, C., Long, D., and Chen, Z., *Russ. J. Appl. Chem.,* 2015, vol. 88, p. 1510.
5. He, Y., Yang, Q., and Xu, Z., *Russ. J. Appl. Chem.,* 2014, vol. 87, p. 1936.
6. Moallem, Z., Danaee, I., and Eskandari, H., *Trans. Indian Inst. Met.,* 2014, vol. 67, p. 817.
7. He, Y., Zhou, Y., Yang, R., Ma, L., and Chen, Z., *Russ. J. Appl. Chem.,* 2015, vol. 88, p. 1192.
8. Liu , X., Lu, Y., Yang, Y.S., Hu, H.X., and Zheng, Y.G., *Russ. J. Appl. Chem.,* 2014, vol. 87, p. 350.
9. Elmsellem, H., Youssouf, M. H., Aouniti, A., Ben Hadda, T., Chetouani , A., and Hammouti, B., *Russ. J. Appl. Chem.,* 2014, vol. 87, p. 744.
10. Liu, X., Cao, H., and Jiang, B., *Russ. J. Appl. Chem.,* 2014, vol. 87, p. 738.
11. Gorbunova, T.I., Bazhin, D.N., Zapevalov, A.Y., and Saloutin, V.I., *Russ. J. Appl. Chem.,* 2013, vol. 86, p. 992.
12. Magerramov, A.M., Bairamov, M.R., Azimova, N.V., Mamedov, I.G., Agaeva, M.A., and Alieva, S.G., *Russ. J. Appl. Chem.,* 2014, vol. 87, p. 456.
13. Danaee, I., Ghasemi, O., Rashed, G.R., RashvandAvei, M., and Maddahy, M.H., *J. Mol. Struct.* 2013, vol. 1035, p. 247.
14. Gürten, A.A., Keleş, H., Bayol, E., and Kandemirli, F., *J. Ind. Eng. Chem.*, 2015, vol. 27, p. 68.
15. Abd El-Lateef, H.M., Abu-Dief, A.M., Abdel-Rahman, L.H., Sañudo, E.C., and Aliaga-Alcalde, N., *J. Electroanal. Chem.,* 2015, vol. 743, p. 120.
16. Chaitra, T.K., Mohana, K.N.S., and Tandon, H.C., *J. Mol. Liq.,* 2015, vol. 211, p. 1026.
17. Ali, O.A.M., *Spectrochim. Acta A*, 2014, vol. 132, p. 52.
18. Gupta, N.K., Verma, C., Quraishi, M.A., and Mukherjee, A.K., *J. Mol. Liq.,* 2016, vol. 215, p. 47.
19. Saha, S.K., Ghosh, P., Hens, A., Murmu, N.C., and Banerjee, P., *Physica E,* 2015, vol. 66, p. 332.
20. Fairhurst, S.A., Hughes, D.L., Kleinkes, U., Leigh, G.L., Sanders, J.R. and Weisner, J., *J Chem. Soc. Dalton Trans.,* 1995, vol. 3, p. 321.
21. Macdonald, J.R., *Solid State Ion.,* 1984, vol. 13, p. 147.
22. Danaee, I., *J. Electroanal. Chem.* 2011, vol. 662, p. 415.
23. Yurt, A., Duran, B., and Dal, H., *Arab. J. Chem.*, 2014, vol. 7, p. 732.
24. Negm, N.A., Ghuiba, F.M., and Tawfik, S.M., *Corros. Sci.*, 2011, vol. 53, p. 3566.
25. Jafari, H., Danaee, I., Eskandari, H., and RashvandAvei, M., *Ind. Eng. Chem. Res.*, 2013, vol. 52, p. 6617.
26. Chetouani, A., Hammouti, B., Benhadda, T., Daoudi, M., *Appl. Surf. Sci.* 2005, vol. 249, p. 375.
27. Chetouani, A., Aouniti, A., Hammouti, B., Benchat, N., Benhadda, T., and Kertit, S., *Corros. Sci.*, 2003, vol. 45, p. 1675.
28. Emeregül, K.C., and Hayval, M., *Corros. Sci.,* 2006, vol. 48, p. 797.
29. Satapathy, A.K., Gunasekaran, G., Sahoo, S.C., Amit, K., and Rodrigues, P.V., *Corros. Sci.,* 2009, vol. 51, p. 2848.
30. Olivares, O., Likhanova, N.V., Gomez, B., Navarrete, J., Llanos-Serrano, M.E., Arce, E., and Hallen, J.M., *Appl. Surf. Sci.*, 2006, vol. 252, p. 2894.
31. Abdel Rehim, S.S., Hazzazi, O.A., Amin, M.A., and Khaled, K.F., *Corros. Sci.*, 2008, vol. 50 p. 2258.
32. Saleh, M.M. and Atia, A.A., *J. Appl. Electrochem.*, 2006, vol. 36, p. 899.
33. Gholami, M., Danaee, I., Maddahy, M.H., and Rashvandavei, M., *Ind. Eng. Chem. Res.,* 2013, vol. 52, p. 14875.
34. Emregül, K.C., and Atakol, O., *Mater. Chem. Phys.,* 2003, vol. 82, p. 188.
35. Li, X.H., Deng, S.D., and Fu, H., *J. Appl. Electrochem.*, 2010, vol. 40, p. 1641.
36. Larabi, L., Harek, Y., Traianel, M., and Mansri, A., *J. Appl. Electrochem.,* 2004, vol. 34, p. 833.
37. Hoseinzadeh, A.R., Danaee, I., and Maddahy, M.H., *J. Mater. Sci. Technol.*, 2013, vol. 29 p. 884.
38. Danaee, I., Gholami, M., RashvandAvei, M., and Maddahy, M.H., *J. Ind. Eng. Chem.,* 2015, vol. 26, p. 81
39. Martinez, S., Metikoš-Hukovic´, M., *J. Appl. Electrochem.,* 2003, vol. 3, p. 1137.
40. Bentiss, F., Lebrini, M., Vezin, H., Chai, F., Traisnel, M., and Lagrené, M., *Corros. Sci.* 2009, vol. 51, p. 2165.
41. Danaee, I., and Noori, S., *Int. J. Hydrogen Energy*, 2011, vol. 36, p. 12102–12111.
42. Karimi, A., Danaee, I., Eskandari, H., and RashvanAvei, M., *Prot. Met. Phys. Chem. Surf.* 2015, vol. 51, p. 899.

43. RameshKumar, S., Danaee, I., RashvandAvei, M., Vijayan, M., *J. Mol. Liq.,* 2015, vol. 212, p. 168.
44. Kumar, C.B.P., Mohana, K.N., *J. Taiwan Institute Chem. Eng.* 2014, vol. 45, p. 1031.
45. Herrag, L., Chetouani, A., Elkadiri, S., Hammouti, B., and Aouniti, A., *Portugal. Ectrochim. Acta*, 2008, vol. 26, p. 211.
46. Jafari, H., Danaee, I., Eskandari, H., and RashvandAvei, M., *J. Mater. Sci. Technol.*, 2014, vol. 30, p. 239.
47. Herrag, L., Hammouti, B., Elkadiri, S., Aouniti, A., Jama, C., Vezin, H., and Bentiss, F., *Corros. Sci.* 2010, vol. 52, p. 3042.
48. Al-Sarawy, A.A., Fouda, A.S., Shehab El-Dein, W.A., *Desalination,* 2008, vol. 229, p. 279.
49. Oguzie, E.E., Unaegbu, C., Ogukwe, C.N., Okolue, B.N., and Onuchukwu, A.I., *Mater. Chem.Phys.,* 2004, vol. 84, p. 363.
50. Hoseinzadeh, A.R., Danaee, I., Maddahy, M.H., Rashvand-Avei, M., *Chem. Eng. Comm.,* 2014, vol. 201, p. 380.
51. Mu, G., Li, X., Qu, Q., and Zhou, J., *Corros. Sci.,* 2006, vol. 48, p. 445.